Environmental Science and Pollution Research (2023) 30:62938–62950
https://doi.org/10.1007/s11356-023-26390-x

RESEARCH ARTICLE

Behavior and mechanisms of ciprofloxacin adsorption on aged polylactic acid and polyethlene microplastics

Jinni Liang[1] · Jiahui Wu[1] · Zhi Zeng[1] · Manzhi Li[1] · Weizhen Liu[2] · Taiping Zhang[1]

Received: 12 December 2022 / Accepted: 7 March 2023 / Published online: 23 March 2023

Abstract

Microplastics (MPs) and antibiotics are emerging pollutants in aquatic environments. MPs can absorb antibiotics, resulting in compound pollution. Batch adsorption experiments were used to investigate the adsorption behavior of CIP on polylactic (PLA) and polyethlene (PE) under various environmental conditions. After a lengthy aging process, both MPs underwent significant physicochemical changes. The equilibrium adsorption capacities of aged PLA and PE were 0.382 mg/g and 0.28 mg/g, respectively, which increased by 18.06% and 75% compared to pristine PLA and PE. The sorption capacity of MPs increased when the pH of the solution approached the dissociation constant (6.09, 8.74) of CIP. When the salinity of the solution was 3.5%, the adsorption capacity of MPs was reduced by more than 65%. The adsorption capacity of MPs rapidly decreased when 20 mg/L fulvic acid was added. Because norfloxacin (NOR) competes for adsorption sites on the microplastic, CIP adsorption is inhibited. Based on the adsorption models, FTIR, and XPS spectra, we demonstrated that the process was monolayer adsorption, with chemical and physical mechanisms including hydrogen bonding, π-π conjugation, ion exchange, and electrostatic interactions controlling it. Thus, PLA and PE microplastics may be a potential vector for CIP in water, and their interaction is mainly influenced by the physicochemical properties of the MPs and environmental factors.

Keywords Aged microplastics · Ciprofloxacin · Emerging pollutants · Adsorption · Vector transport · Degradable

Introduction

Plastic is a polymer that has high chemical stability and plasticity. As a result, it is widely used in many fields of industry and life (Andrady 2011). In the previous 60 years, plastic manufacturing has grown 622-fold, from 500,000 to 311 million tons (Thompson et al. 2009). Polyethlene accounts for most synthetic resin plastics worldwide, i.e., 36% of the total production (Geyer et al. 2017). Biodegradable plastics were developed to minimize the environmental damage caused by traditional plastics. The annual biodegradable plastic production is gradually increasing. In 2025, it was predicted to reach 2.4 million tons (Polman et al. 2021). PLA is the most common biodegradable plastic used in industry. Its output will rise from 30×10^4 t per year to 95×10^4 t per year over the next ten years (Shruti and Kutralam-Muniasamy 2019). However, degradable plastics can only be wholly degraded under particular conditions. Degradable plastics are more likely to produce microplastics and adsorb other pollutants, which may have a bigger negative impact on the environment.

Responsible Editor: Tito Roberto Cadaval Jr

✉ Taiping Zhang
lckzhang@scut.edu.cn

Jinni Liang
1061586191@qq.com

Jiahui Wu
1404673226@qq.com

Zhi Zeng
1539724995@qq.com

Manzhi Li
1310951436@qq.com

Weizhen Liu
weizhliu@scut.edu.cn

[1] School of Environment and Energy, South China University of Technology, Guangzhou 510006, People's Republic of China

[2] Guangdong Provincial Key Laboratory of Solid Wastes Pollution Control and Recycling, South China University of Technology, Guangzhou, Guangdong 510006, People's Republic of China

Previous research has revealed that only a tiny proportion (6 to 26%) of plastic trash gets recycled. As a result, a considerable amount of plastic waste leads to environmental pollution (Alimi et al. 2018). According to some researchers, if the production of plastics continues to rise and plastic trash is not effectively treated, by the middle of the twenty-first century, approximately 12 billion tons of plastic trash will be stored in the natural environment (Jambeck et al. 2015). Plastic breaks down into pieces in the environment by abrasion, oxidation, hydrolysis, photoaging, and biological action of traditional and biodegradable plastic waste (Horton et al. 2017). Plastic fragments smaller than 5 mm are usually referred to as MPs internationally to unify the definition (Bakir et al. 2014). Microplastic pollution in oceans, lakes, and rivers has become more widespread (Campanale et al. 2020; Ding et al. 2019; Sighicelli et al. 2018). The primary source of microplastics in the environment is the crushing process of large plastic products. Furthermore, the release of microplastics into the environment by industrial and domestic wastewater should not be overlooked. Microplastic bioaccumulation along the food chain can occur in aquatic systems, affecting individuals and populations. Microplastics can potentially cause a wide range of toxicological reactions in organisms, including lethality, reduced feeding activity, growth and development inhibition, endocrine disruption, disruption of energy metabolism, oxidative stress, immune and neurotransmission dysfunction, and even genotoxicity (Lu et al. 2016). Because of their large specific area, hydrophobicity, and mobility, microplastics can accumulate chemical contaminants and act as carriers for long-distance transportation (Guo et al. 2012). Frias et al. (2010) reported that persistent organic pollutants such as polycyclic aromatic hydrocarbons, polychlorinated biphenyls, and dichlorodiphenyltrichloroethane were found in microplastic particles collected from two beaches in Portugal. Some scholars dispersed microplastics along the Chinese coastline in various locations. Six months later, heavy metals such as chromium, lead, and manganese were discovered on these microplastics (Gao et al. 2019). Qiao et al. (2019) demonstrated that the presence of MPs can extend other pollutants' half-lives, enhance their bioavailability, and increase toxicity to organisms. Hence, it is crucial to comprehend the mechanisms and processes involved in MPs' pollutant adsorption.

As a new category of pollutants, antibiotics have attracted considerable interest due to their impact on biology and the generation of medicine-resistance genes (Yang et al. 2017). From 2000 to 2015, global antibiotic consumption grew by 69% (Klein et al. 2018). The intestines of humans and animals are not very efficient in absorbing antibiotics. As a result, most antibiotics are excreted directly into the environment as prodrugs (Danner et al. 2019). Li et al. (2018) examined 27 antibiotic residues in the Pearl River coastal area, among which macrolides were the most abundant, with 217 ng/L in river water and 232 ng/L in seawater. Sulfonamide antibiotics are incredibly stable and do not degrade easily in the environment. Aquatic organisms exhibit chronic toxicity due to long-term antibiotic contamination (Wang et al. 2019). Studies have revealed that antibiotics can change the structure and variety of microbial communities by impeding processes like enzyme activity and food uptake. Additionally, antibiotics in the environment can result in the development of antibiotic-resistance genes (ARGs) and resistant flora. The presence of ARGs can render antibiotics useless, impair their ability to treat the disease effectively, and endanger human health (Grenni et al. 2018). If antibiotics were enriched on microplastics, producing combined pollution, they might cause more significant harm to the environment and organisms. When aquatic organisms are exposed to a combination of antibiotics and microplastics, their bodies become enriched with microplastics. Antibiotics are transported from microplastics to organisms via desorption in the intestines of the organisms, causing harm to the organisms (Razanajatovo et al. 2018). When both microplastics and antibiotics are present in the environment, the two contaminants can interact physically and chemically. This allows microplastics to act as antibiotic carriers, transporting them through the water to different locations (Atugoda et al. 2020). Understanding the mode and mechanism of interaction between microplastics and antibiotics can thus aid in investigating microplastics' vector transport effect and possible environmental dangers of co-occurring antibiotics.

Antibiotic sorption studies on microplastics had primarily focused on conventional microplastics. Studies on the sorption behavior of antibiotics by biodegradable microplastics have begun as the use of biodegradable plastics has increased. However, there has been no comparative research on the interactions of conventional and biodegradable microplastics with antibiotics. Plastic aging can cause changes in the physicochemical properties of plastics, affecting their ability to adsorb other contaminants. Most previous studies used a single aging treatment, such as UV radiation (Zheng et al. 2023). Simple aging treatments do not replicate the effects of complex environmental conditions in nature on microplastic aging. Furthermore, the interaction of MPs with other contaminants may be influenced by complex environmental factors. Despite the fact that many studies have reported that antibiotics can be adsorbed by various microplastics, there has been little research on the mechanism of interaction between antibiotics and microplastics, as well as the effect of pH, dissolved organic matter, and ionic strength on their adsorption capacity.

PLA is a new biodegradable plastic, while PE is a traditional plastic. These two types of plastic are commonly found in everyday life. Aged and new PLA/PE were used in our experiments. CIP was selected as an example to

investigate the adsorption of microplastics. The objectives of this research were to investigate (1) how aging affects microplastic characteristics and adsorption performance, (2) the adsorption mechanisms of CIP on PLA and PE using the kinetic model, isotherm models, and thermodynamics, and (3) the effects of temperature, pH, ionic strength, fulvic acid, and norfloxacin (NOR) on the adsorption.

Materials and methods

Materials and reagents

Zhongxin Plastics Limited Company (Dongguan, China) provided PLA and PE. Supplementary Table S1 describes the specific physicochemical characteristics of MPs. McLean Biochemical Technology Co., Ltd. supplied the CIP (purity ≥ 98%), NOR (purity ≥ 98%), methanol, and acetic acid. Guangzhou Chemical Reagent Factory supplied sodium chloride (NaCl), sodium hydroxide (NaOH), sodium persulfate ($Na_2S_2O_8$), hydrochloric acid (HCl), fulvic acid (purity ≥ 85%), and sulfuric acid (H_2SO_4). Methanol and acetic acid were chromatography grade, and the remaining chemicals were analytically pure grade. To prepare a stock solution, the CIP was dissolved in a small amount of acetic acid and then diluted with ultrapure water. Keep the stock solution in the fridge at 4 °C. Before using, dilute it to the required concentration.

Preparation of aged PLA and PE

In the environment, microplastics typically suffer natural erosion. Microplastics were exposed to acid corrosion, alkali corrosion, UV-activated persulfate oxidation, freezing, and heating to simulate the aging effects of complex environmental conditions in nature. First, 50 g of microplastic was placed in 500 ml of 1 mol/l H_2SO_4. Microplastics float on the water's surface due to their low density. As a result, it was placed on a magnetic stirrer to ensure complete contact with the solution. After seven days, it was filtered, neutralized with pure water, and placed in 500 ml of 1 mol/l NaOH. Similarly, it was placed on a magnetic stirrer for seven days to ensure that the microplastic and NaOH made complete contact. They were then filtered and rinsed to neutrality before being placed in 500 ml of 0.1 mol/l $Na_2S_2O_8$ and stirred for seven days under UV light irradiation at 50 W/m^2. Finally, they were frozen at − 20 °C for 12 h and heated at 70 °C for 12 h. This freezing and heating cycle lasted for seven days. After the treatment, all aged microplastic particles were washed and dried.

Characterization

A scanning electron microscope (SEM, TESCAN MIRA LMS, Czech Republic) was used to examine the surface characteristics of the microplastics. N2 adsorption–desorption analysis (Micromeritics APSP 2460, Conta Instruments, USA) was performed at 77 K to calculate the surface area and pore volume of MPs. To define the adjustments in exterior functional groups of MPs before and after the aging process or adsorption, Fourier transforms infrared spectroscopy (FTIR, Nicolet iS 10, Thermo-Nicolet, USA) and X-ray photoelectron spectroscopy (XPS, D8 ADVANCE, Bruker, Germany) were used. A contact angle tester (JY-82B Kruss DSA, China) was used to measure the contact angle of microplastics.

CIP determination

High-performance liquid chromatography (HPLC, Agilent 1200, USA), C18 column, at a wavelength of 278 nm, was used to quantify the samples. The instrument's column temperature was set to 30 °C. The mobile phase was 68:32 (v: v) 5% acetic acid and methanol at a flow rate of 1 mL/min; the sample injection volume was set to 20 μL each time.

Adsorption experiments

To conduct kinetic adsorption experiments, 200 mg of MPs (100 μm) and 40 ml of 3 mg/L CIP solution were added into 40 mL brown conical flasks. Bottles were placed on a shaker with an air bath (Xinmiao Medical Equipment Manufacturing Co., Ltd., Shanghai, China). The shaker was set to 298 K and 180 rpm. Between 0 and 96 h, samples were taken in intervals. HPLC was used to determine the concentration of CIP after the supernatant had been filtered through a 0.22 μm nylon membrane (nylon 6, Jinteng, China) filter to remove MPs. The initial concentration of CIP in the adsorption isotherm studies varied from 1 to 5 mg/L. Adsorption experiments were performed at 288 K, 298 K, and 308 K, respectively. To determine how PH affects adsorption, the pH of the 3 mg/L CIP solution was adjusted to 3, 5, 7, 9, and 11 using 0.1 M NaOH and HCl, respectively. Varying the NaCl mass fraction (0–3.5%) results in different ion concentrations, and the effect of varying ion concentrations on CIP adsorption by microplastics was studied. Additionally, fulvic acid solutions in various concentrations (0–20 mg/L) and NOR solutions (1–5 M) were used to create CIP solutions (3 M). The sample solutions were filtered through 0.22 μm filters and analyzed with HPLC after 24 h. Experiments were performed in duplicate. Data were presented as means and standard deviations.

Sorption and thermodynamic models

The experimental results were interpreted using the Lagergren pseudo-first-order (Eq. 1), Lagergren pseudo-second-order (Eq. 2), and Webber-Morris models to gain insights into the kinetic mechanisms of CIP adsorption on MPs (Eq. 3)

$$q_t = q_e(1 - e^{-k_1 t}) \tag{1}$$

$$q_t = \frac{k_2 q_e^2 t}{1 + k_2 q_e t} \tag{2}$$

$$q_t = k_{ti} t^{\frac{1}{2}} + C \tag{3}$$

where the theoretical adsorption capacity of the adsorbent at equilibrium is represented by q_e (mg/g). The adsorption time is given by t (min), and the adsorption capacity at time t is given by q_t (mg/g); k_1 (1/min) is the Lagergren pseudo-first-order, and k_2 (g/(mg-min)) is Lagergren pseudo-second-order kinetic reaction rate constants, respectively; k_{ti} (mg/(g-min$^{1/2}$)) is the intraparticle diffusion constant; and C is the associated constant boundary layer thickness.

The Freundlich model (Eq. 4), Langmuir model (Eq. 5), and Hill model (Eq. 6) were applied to analyze the adsorption isotherm to elucidate adsorption properties further.

$$q_e = K_f \times C_e^{1/n} \tag{4}$$

$$q_e = \frac{q_m \times C_e}{K_L + C_e} \tag{5}$$

$$q_e = \frac{q_m (K_h C_e)^b}{1 + (K_h C_e)^b} \tag{6}$$

where q_e (mg/g) and q_m (mg/g) are the adsorption mass at equilibrium and the theoretical saturation per unit adsorbent, respectively; the mass concentration of the adsorbate is expressed by C_e (mg/L) as its adsorption equilibrium value; K_F is the Freundlich adsorption constant; K_L (L/mg) is the Langmuir adsorption constant; and n is the Freundlich constant. $1/n$ is related to the adsorption surface heterogeneity. When $0 < 1/n < 1$, the adsorption is readily occurring. When $1/n = 1$, there is a lack of interaction between adsorbate and adsorbed material, and adsorption is homogeneous. When $1/n > 1$, adsorption is not readily occurring. For the Hill model, K_h is the Hill's constant and b is the Hill coefficient of cooperation. A parameter b greater than 1 corresponds to a positive interaction.

The following equations were used for the thermodynamic study.

$$\triangle G = -\mathrm{RT} \ln K_C \tag{7}$$

$$K_C = \frac{Q_e}{C_e} \tag{8}$$

$$\ln K_C = \frac{\triangle S}{R} - \frac{\triangle H}{RT} \tag{9}$$

where ΔS (J/mol) is entropy; ΔH (J/mol) is enthalpy; ΔG (J/mol-K) is the Gibbs-free energy; t (K) is the temperature of the reaction system; R (8.314 J/ (mol K) is the gas constant; and K_C (mL/g) is the partition coefficient of the adsorbate in the solid–liquid phase.

Results and discussion

Physical and chemical property changes

Figure 1 shows the morphologies of the new and old MPs. The figure shows that the new PLA surface had some folds and pits, while the new PE surface was comparatively regular and flat. After extensive aging treatment, aged PLA and PE surfaces became rougher. Moreover, the surface morphology of PLA and PE changed differently after aging. The aged PLA surface had many small and deep holes, whereas the aged PE surface had more cracks. Cracks and pits were discovered in the surface properties of aged MPs. This is a suitable condition for molecular diffusion while providing a larger surface area for CIP adsorption by MPs (Kannaujiya et al. 2023). In the current study, the surface morphology of aged MPs showed cracks and pits similar to previously reported characteristics of aged MPs (Li et al. 2018). Supplementary Table S1 displays the specific surface areas (SSA), total pore volumes, and contact angles of pristine and aged MPs. Before aging, the SSA of PLA and PE were 1.7915 m^2/g and 0.6978 m^2/g. The SSA of aged PLA and PE reached 4.2525 m^2/g and 1.0016 m^2/g, which was 2.4 and 1.4 times higher than before aging. The total volume of PLA also increased by a factor of 1.57 due to aging. However, the total PE volume did not change much due to aging. Theoretically, an adsorbent with a larger surface area and pore volume can capture more pollutants (Zhou et al. 2020). The contact angles of PLA and PE decreased by 1.34° and 3.53°, respectively, due to aging, and the hydrophobicity decreased.

Figure 2 depicts the FTIR spectrum of new and aged microplastics. For aged PLA, the peak intensities at 1752 cm^{-1}, 3450 cm^{-1}, and 3666 cm^{-1} increased. These peaks correspond to C = O, O–H, and free O–H, respectively. For aged PE, a significant decrease in peak intensities was observed at 2920 cm^{-1} and 1462 cm^{-1}. These peaks correspond to the functional groups C = H and C-H, respectively.

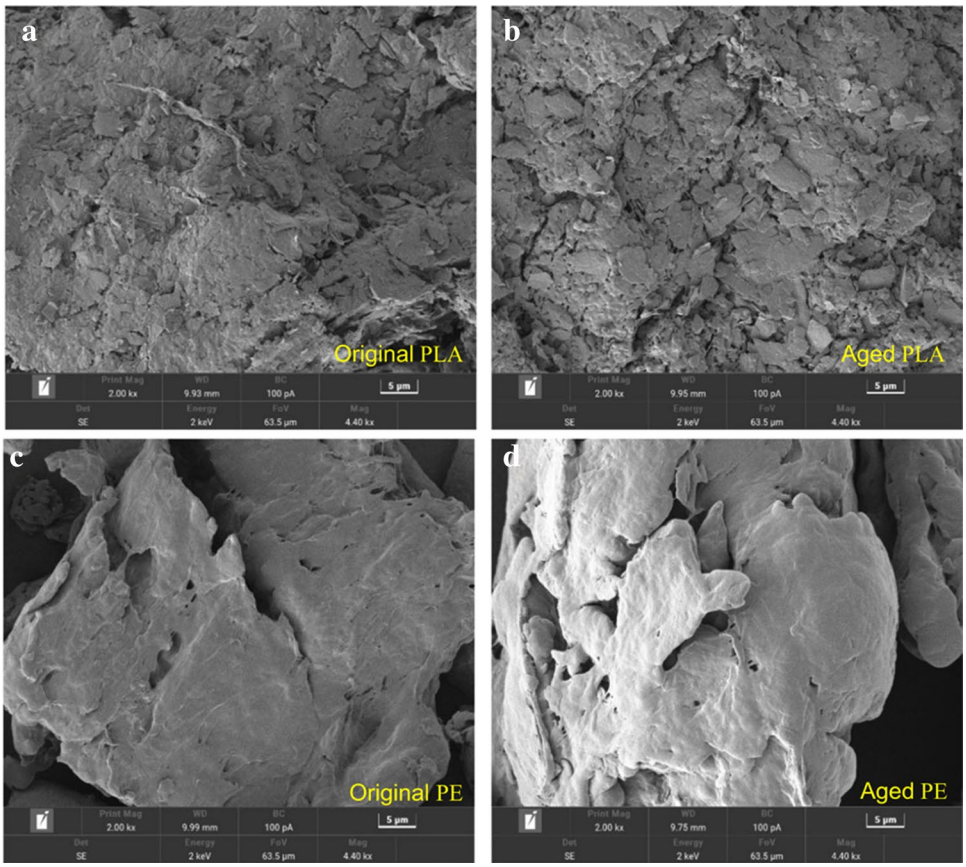

Fig. 1 SEM images of original PLA (**a**), aged PLA (**b**), original PE (**c**), and aged PE (**d**)

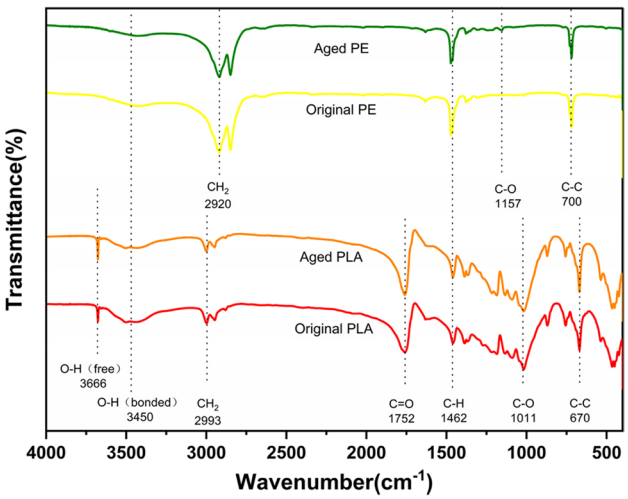

Fig. 2 FTIR spectra of microplastics before and after the aging process

The peak intensity increased at 3450 cm^{-1}, and there was a new peak at 1157 cm^{-1}, corresponding to O–H and C-O. The breakdown of the C-H bond and subsequent interaction with oxygen to produce peroxyl radicals may have caused the increase in oxygen-containing functional groups (C-O). Peroxyl radicals can take up hydrogen atoms from their surroundings, creating hydrogen peroxide groups (COOH), which then break down further to generate additional functional groups (C = O, C–OH) (Yousif and Haddad 2013). The complex aging process introduces enough oxygen-containing acidic functional groups on its surface. It has been shown that these oxygen-containing functional groups can trap some cations in solution (Khandaker et al. 2021). The strength of oxygen-containing functional groups, such as hydroxyl and carbonyl groups, increases with age, which can affect the hydrophilicity of MPs (Huang et al. 2020). In previous research, the contact angle of aged MPs was reduced, demonstrating that aging enhances the hydrophilicity of MPs.

Adsorption kinetics

The kinetics of CIP adsorption on the four MPs (Fig. 3a) revealed that the adsorption rate of MPs seemed to be initially high, then gradually decreased, and 90% of the CIP adsorption capacity of the four microplastics was reached in 12 h. The rapid increase of the adsorption rate in the early stage of the adsorption process proved the intense attraction between MPs and CIP, revealing that the surface of MPs has sufficient adsorption sites (Hasan et al. 2023). The

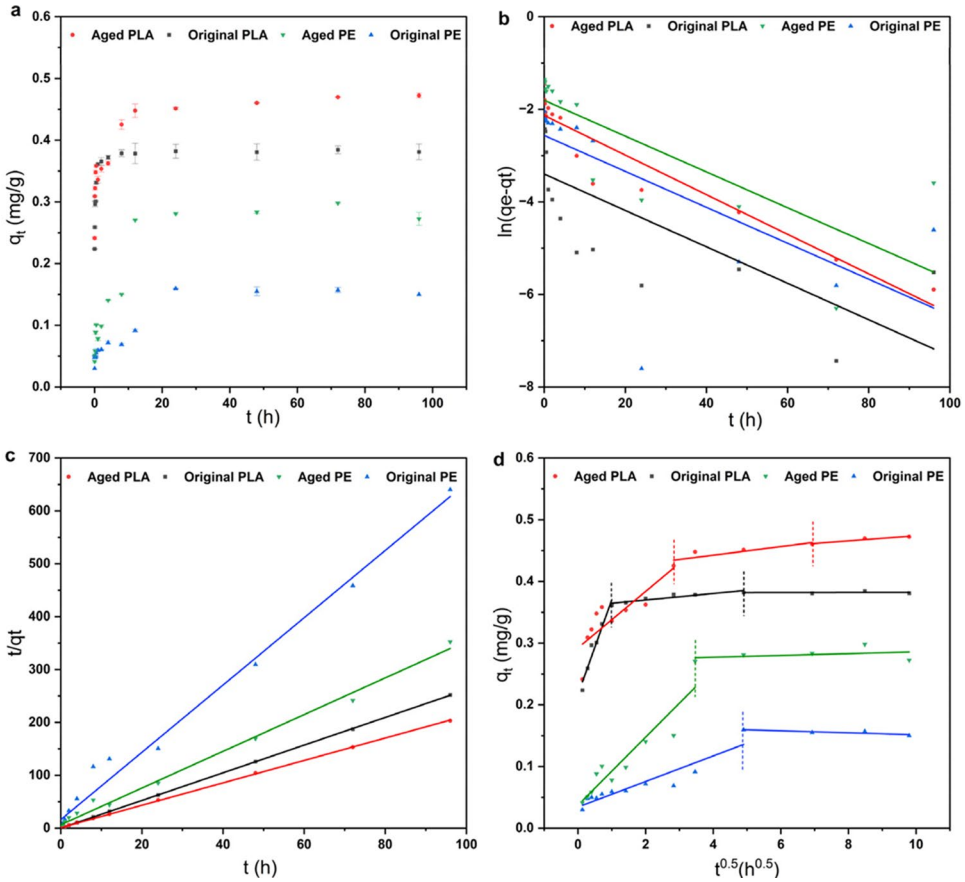

Fig. 3 (**a**) CIP adsorption by MPs, (**b**) Lagergren pseudo-first-order model, (**c**) Lagergren pseudo-second-order model, and (**d**) Webber-Morris model

massive accumulation of CIP on MPs reduces the number of active available sites, and adsorption gradually tends to dynamic equilibrium (Kannaujiya et al. 2021). The adsorption reached dynamic equilibrium after shaking for 24 h. The adsorption capacities of pristine PLA, aged PLA, pristine PE, and aged PE were 0.382 mg/g, 0.451 mg/g, 0.16 mg/g, and 0.28 mg/g, respectively. The remaining concentrations of pollutants in the sample after treatment were 1.09 mg/L, 0.745 mg/L, 2.36 mg/L, and 1.6 mg/L, respectively. The four MP adsorption kinetic curves were nearly identical, but their equilibrium adsorption capacities decreased in the following order: aged PLA > PLA > aged PE > PE.

The adsorption kinetic values were compared using Eqs. (1)–(4) to investigate adsorption mechanisms and clarify the adsorption behavior. The R^2 of the Lagergren pseudo-second-order model is greater than 0.987, as shown in Table 1. The Lagergren pseudo-second-order model has a higher R^2 than Lagergren pseudo-first-order model. The q_e derived from the Lagergren pseudo-second-order model, and the actual situation differed significantly. As a result, the Lagergren pseudo-second-order was better suited to describe MP adsorption behavior for CIP, which was primarily governed by chemisorption (Bao et al. 2021). Furthermore, the specific adsorption process of CIP on MPs was investigated by fitting the experimental data to the Webber-Morris model (Fig. 3d, Supplementary Table S2). There are multiple levels and no linear connection between q_t and $t^{0.5}$ in their functional relationship. MPs adsorption process comprised two or more stages. This means that the adsorption rate of microplastics is determined by external diffusion as well as

Table 1 Lagergren pseudo-first-order model and Lagergren pseudo-second-order model parameters for CIP adsorption on microplastics

MPs	Lagergren pseudo-first-order model			Lagergren pseudo-second-order model		
	q_e (mg/g)	k_1 (1/min)	R^2	q_e (mg/g)	k_2 (g/(mg-min))	R^2
Original PLA	0.049	0.091	0.492	0.382	22.84	0.9997
Aging PLA	0.137	0.099	0.897	0.472	4.275	0.9999
Original PE	0.050	0.089	0.413	0.157	2.503	0.9872
Aging PE	0.122	0.089	0.60	0.288	1.872	0.9926

intraparticle diffusion (Bhattacharyya and Sharma 2004). The adsorption process of PLA involves three periods, i.e., the surface diffusion period, the mesoporous adsorption period, and the micropore adsorption period. However, the adsorption process of PE involved only two periods, i.e., the surface adsorption period and the mesoporous adsorption period. This could be because PLA contains micropores while PE contains only a few larger voids. The adsorption rate of PLA diminished in the order of $K_{ip1} > K_{ip2} > K_{ip3}$, and that of PE in the order of $K_{ip1} > K_{ip2}$. Finally, the chemisorption of CIP on MPs was governed by both inside and outside diffusion processes.

Adsorption isotherms

Figure 4 and Supplementary Fig. S1 show the adsorption isotherms of CIP on PLA, aged PLA, aged PE, and PE. The outcomes of the Langmuir, Freundlich, and Hill models are shown in Table 2. At different temperatures, the adsorption capacity of four microplastics for CIP differed significantly. The increase in temperature is beneficial to the adsorption of antibiotics by microplastics. The adsorption of the four MP isotherms was nonlinear, suggesting that MP adsorption efficiency was related to CIP concentration.

The adsorption isotherm is used to analyze the interaction between the adsorbent and the adsorbed molecule, as well as the adsorption properties. The R^2 of the models was higher than 0.90. The Langmuir model fitted the data slightly better than the Freundlich model. Based on the basic assumptions of the models, it could be deduced that the adsorption of CIP on the four MPs was monolayer. The q_m of aged MPs was greater than unaged MPs, indicating that aged MPs had increased adsorption performance than new MPs. All K_F and n results demonstrated that PLA attracted CIP more strongly than PE (Fan et al. 2021; Jiang et al. 2020). From the Hill model, the interaction between CIP and microplastics can be interpreted as a cooperative adsorption process. The binding of CIP and specific sites on microplastics influences the binding ability of other sites on the microplastics' surface (Ashiq et al. 2019). The value of b for aged PLA is greater than one, indicating that the interaction between CIP and aged PLA is always cooperative. The remaining three microplastics, on the other hand, interacted with CIP in both positive and negative cooperative binding. This may be due to intermolecular forces. At different temperatures, the CIP molecules adsorbed on the microplastics exert repulsive or attractive forces on the surrounding dispersed CIP molecules. Furthermore, the positive k_h values demonstrate that

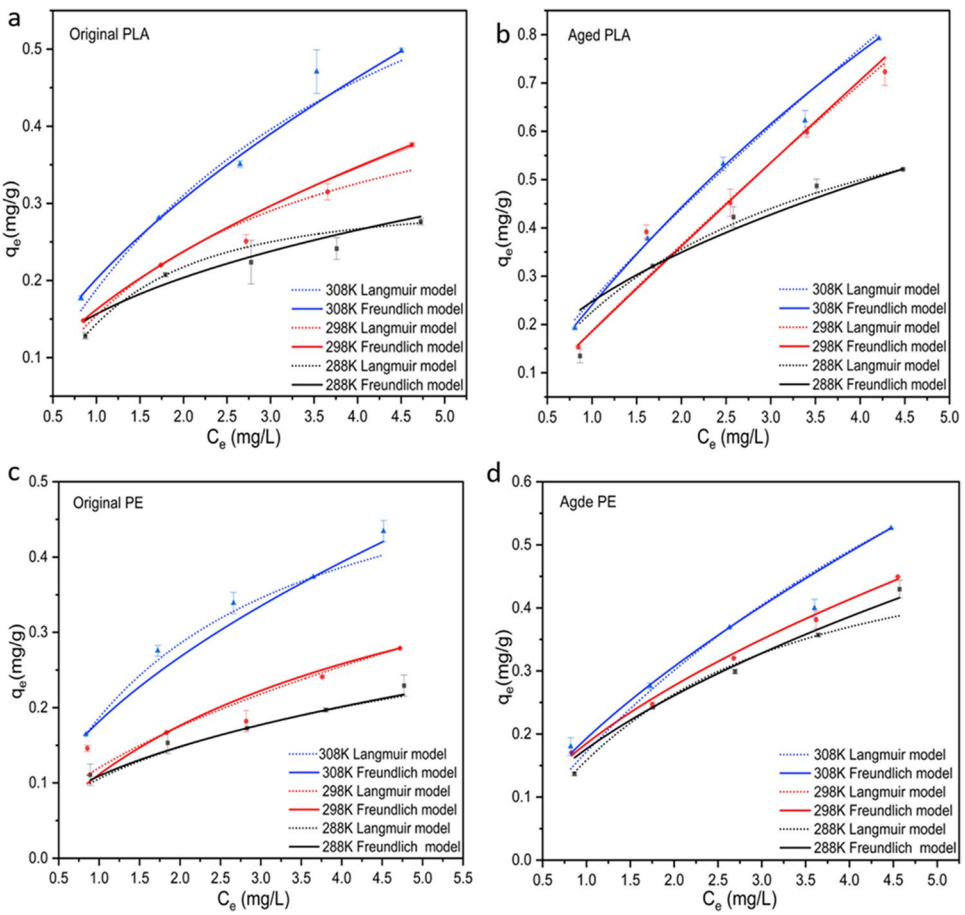

Fig. 4 Adsorption of CIP on microplastics as fit to Langmuir and Freundlich models

Table 2 The Langmuir, Freundlich, and Hill isotherm model parameters for CIP adsorption on microplastics

MPs	Temperature k	Langmuir			Freundlich			Hill		
		q_m (mg/g)	k_L (L/mg)	R^2	n	k_F (L/mg)	R^2	n	k_h (L/mg)	R^2
Original PLA	288	0.3063	0.8844	0.9895	2.617	0.1562	0.9026	1.669	0.1672	0.9895
	298	0.5168	0.4269	0.9620	1.821	0.1623	0.9979	0.6597	0.9856	0.9970
	308	0.6367	0.014	0.9968	1.669	0.202	0.9979	0.5377	0.2560	0.9967
Aging PLA	288	0.837	0.370	0.9968	2.007	0.2473	0.9936	2.2049	0.502	0.9999
	298	1.256	0.248	0.9710	1.037	0.1856	0.9694	2.0317	0.0881	0.9842
	308	2.586	0.0945	0.9993	1.230	0.2499	0.9989	1.2065	0.7938	0.9996
Original PE	288	0.2838	0.1829	0.9595	2.242	0.1093	0.9822	1.039	0.6921	0.9592
	298	0.4803	0.2376	0.9997	1.843	0.1202	0.9999	0.6309	0.7072	0.9998
	308	0.5951	0.4577	0.9999	1.796	0.1818	0.9999	1.5147	0.2112	0.9999
Aging PE	288	0.5357	0.4197	0.9882	1.771	0.1765	0.9616	1.4257	0.6334	0.9883
	298	0.9786	0.0046	0.9950	1.724	0.1850	0.9968	0.7323	0.4514	0.9952
	308	1.462	0.133	0.9999	1.493	0.1931	0.9999	1.4209	0.3923	0.9999

hydrophobic and electrostatic interactions are important in the adsorption process (Sarici ÖzdemİR 2018).

Adsorption thermodynamics

Supplementary Table S3 gives the thermodynamic parameters of adsorption. At various temperatures, ΔG was greater than zero. All four MPs must absorb external energy to facilitate the adsorption reaction. Positive ΔH values for the four MPs supported this conclusion and were consistent with the results of isotherm experiments. The increase in experimental temperature shifted the equilibrium toward heat absorption, which favored adsorption.

Environmental factors

pH

The adsorption process exhibited a significant dependence on pH (Fig. 5a), with the greatest capacity for adsorption at pH 7. This adsorption behavior can be explained by the morphology of CIP at different pH values. pKa_1 (6.09) and pKa_2 (8.74) were the two isoelectric points of CIP (Changfu et al. 2022). Previous studies showed that PLA was usually negatively charged on the surface at pH 3–12 (Sun et al. 2021). PE, however, was positively charged (Sun et al. 2022). At low pH values (< 6.09), electrostatic interactions occur between the cationic form of CIP and PLA. At this point, additional H^+ in the solution competes with CIP, reducing the amount of CIP adsorbed by PLA. However, there was a little difference in the amount of PLA adsorbed to CIP between pH = 3 and PH = 7, indicating that chemisorption was not negligible. PE was positively charged at lower pH values. A repulsive force between PE and CIP occurred due to electrostatic interaction, inhibiting adsorption. At pH values between 6.09 and 8.74, CIP existed as amphiphilic ions, and both electrostatic and hydrophobic effects played a crucial function around the neutral condition (Naushad et al. 2019). CIP occurred primarily in the anionic form at pH values > 8.74. Because of the negative surface charge of PLA, electrostatic repulsion suppressed CIP adsorption. Conversely, electrostatic attraction enabled PE to absorb CIP. However, as the amount of OH- in solution rose, it battled for adsorption sites with CIP, causing a reduction in CIP adsorption efficiency. Thus, the adsorption mechanism between CIP and MPs was controlled by a combination of electrostatic, chemical, and hydrophobic interactions. Because natural water bodies provide an environment with a pH close to neutral, microplastics have a high potential for CPX transfer via adsorption.

Salinity studies

As shown in Fig. 5b, the adsorption capacity of MPs decreased as salinity rose. During this study, the adsorption capacities of pristine PLA, aged PLA, pristine PE, and aged PE were 0.0573 mg/g, 0.1330 mg/g, 0.050 mg/g, and 0.058 mg/g, respectively. With that, without Na^+, the adsorption capacities were reduced by 84.23%, 70.35%, 67.21%, and 78.03%, respectively. This demonstrated that CIP adsorption on MP was linked to the ionic exchange. The increase in salinity inhibits the accumulation of CIP on MPs, which is probably due to the competition between Na^+ and CIP cations to adsorb to the limited active site on the MPs (Jabar and Odusote 2020). At the same time, the rise in NaCl concentration led to the salt precipitation of CIP, and the aggregated CIP was difficult to approach MPs (Yu et al. 2020).

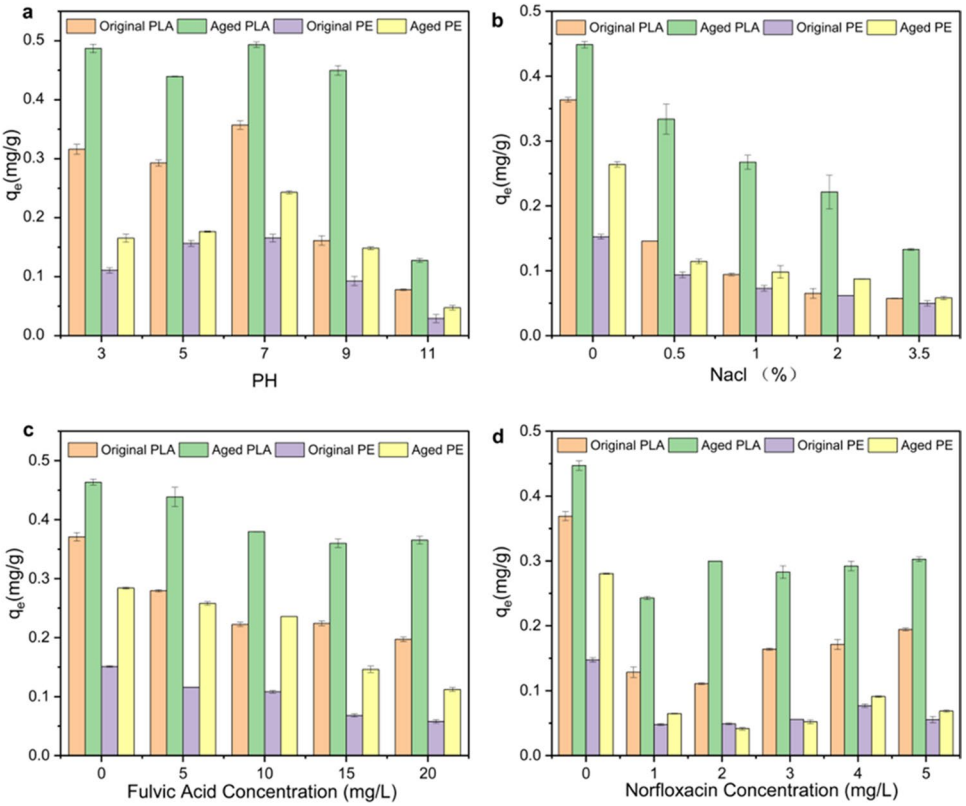

Fig. 5 Effect of pH (**a**), Na^+ (**b**), fulvic acid concentration (**c**), and coexisting norfloxacin on CIP adsorption on microplastics (**d**)

Fulvic acid

As illustrated in Fig. 5c, the adsorption of CIP by the four MPs was significantly inhibited within the tested fulvic acid concentration range. The adsorption capacity of new PLA, aged PLA, new PE, and aged PE was reduced by up to 46.85%, 21.18%, 61.59%, and 60.56% when the fulvic acid concentration was 20 mg/L, respectively. It indicated the existence of competitive adsorption interactions between antibiotics and fulvic acid on the MPs. The reasons for that were (1) the presence of fulvic acid may alter the partitioning of CIP between MPs and water. CIP and fulvic acid have a high affinity for complexation, which hinders MP adsorption (Liu et al. 2017). (2) Fulvic acid can bind to the carboxyl functional groups and hydrogen bonds on the surface of microplastics, reducing the number of adsorption sites on MPs. Meanwhile, the electrostatic field created by the fulvic acid molecules was adsorbed on the microplastics, causing it difficult for CIP to move closer to microplastics (Fu et al. 2013).

Coexisting norfloxacin

To clarify the effect of similar antibiotics, the adsorption of CIP on MPs at different concentrations of NOR (0–5 mg/L) was investigated. The adsorption capacity is shown in Fig. 5d. For new PLA and aged PE, the adsorption capacity of CIP significantly decreased with increasing NOR concentration in the range of 0–2 mg/L. Since the NOR concentration rose from 3 to 5 mg/L, the adsorption capacity gradually increased. For aged PLA and new PE, the adsorption capacity initially decreased (0–1 mg/L) and then slowly increased (2–5 mg/L) with NOR concentration. With NOR, the adsorption capacity of MP for CIP was lower than without NOR, and the presence of NOR negatively affected the adsorption of CIP by MP. NOR inhibited the adsorption of CIP more strongly at low concentrations ($C_{NOR} < C_{CIP}$). Previous research has revealed that certain antibiotics fight for the same functional groups. As a result, one antibiotic may be able to decrease the adsorption affinity of another (Ma et al. 2021).

Adsorption mechanisms

The influence of environmental factors on adsorption performance shows that the maximum capacity of CIP on MPs was found at pH = 7 when salinity was 0; there was no humic acid and norfloxacin present. CIP adsorption on microplastics is mainly reliant on electrostatic and hydrophobic effects at pH = 7, where CIP exists as amphiphilic ions (Jabar et al. 2022; Jabar and Odusote 2021). Adsorption inhibition was observed when NaCl was added to the adsorption system. This observation suggests that ion exchange is important in the mechanism

of CIP adsorption by microplastics. The binding of CIP and HA by intermolecular forces prevents CIP adsorption by microplastics. On both HA and NOR, specific functional groups exist that can compete with CIP for adsorption sites on MPs (Zuo et al. 2019). Figures 6 and 7 showed FTIR and XPS measurements to further elaborate the mechanism of CIP adsorption on MPs. The intensity of O–H (3676, 3474) and C = O (1752) stretching vibration peaks showed a decreasing trend in fresh and aged PLA after adsorption compared to before adsorption, indicating that hydrogen bonding and π-π conjugate bonding played a vital role in adsorption (Xiong et al. 2020). The intensity of CH_2 (2914), C-H (1467), and C–C (711) stretching vibration peaks increased after the adsorption of CIP for both new PE and aged PE, indicating that π-π conjugate bonds determined their adsorption processes. The XPS spectra in Fig. 7 further reveal the mechanism of CIP adsorption by MP. After

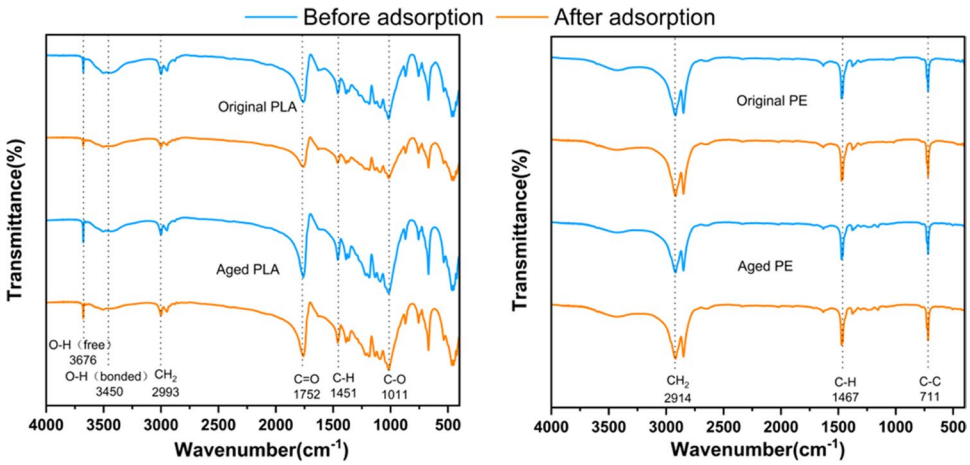

Fig. 6 FTIR spectra of microplastics before and after CIP adsorption

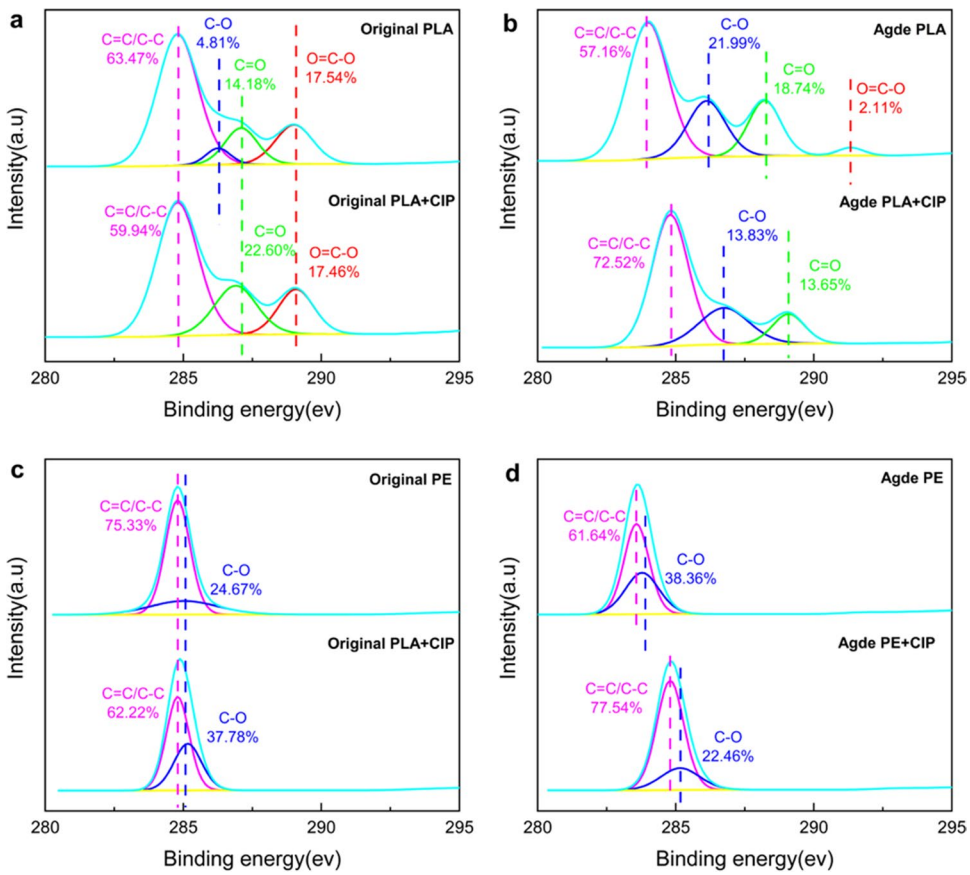

Fig. 7 XPS spectra of microplastics before and after CIP adsorption

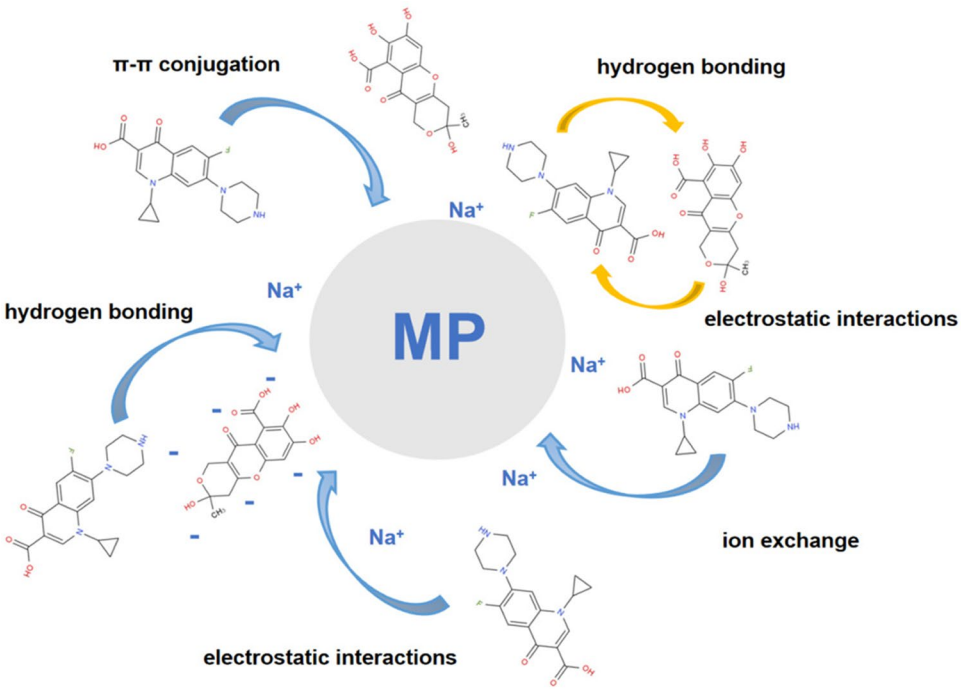

Fig. 8 Adsorption mechanism of CIP on MPs

adsorption, the percent of C = C/C–C of PE rose, implying that π-π is crucial in adsorption. The percent of surface O-including functional groups is bigger in aged MP. The oxidation of exterior groups imparted hydrophilicity on the plastic surface and enhanced the tendency of CIP adsorption on the MPs (Zhang et al. 2018). In summary, the adsorption of CIP on MP is a mix of chemical and physical interactions. Chemical interactions included hydrogen conjugation, π-π bonding, and ion exchange. Electrostatic interactions and electrostatic repulsion were examples of physical interactions (Fig. 8).

Conclusions

To better understand the possibility of synergistic transport of microplastics as antibiotic carriers in an aqueous environment, the differences in CIP adsorption behavior of virgin and aged plastics were investigated in this study using the conventional plastic PE and the biodegradable plastic PLA as adsorbents. After a lengthy aging process, both microplastics underwent significant physicochemical changes. The equilibrium adsorption capacities of aged PLA and PE were 0.382 mg/g and 0.28 mg/g, respectively, which increased by 18.06% and 75% compared to pristine PLA and PE. The four MPs' adsorption data corresponded well with the Lagergren pseudo-second-order kinetic and Langmuir isotherm models, which were primarily governed by monolayer chemisorption. The adsorption process was a non-spontaneous heat absorption reaction. The degree of CIP adsorption by microplastics is affected not only by temperature, concentration, and microplastic physicochemical properties but also by matrix effects (pH, salinity, fulvic acid, and similar antibiotics). When the solution's pH was close to the dissociation constant (6.09,8.74) of CIP, the sorption capacity of MPs increased. When the solution salinity was 3.5%, the adsorption of microplastics to CIP decreased by more than 65%. The adsorption capacity of new PLA, aged PLA, new PE, and aged PE was reduced by up to 46.85%, 21.18%, 61.59%, and 60.56% when the fulvic acid concentration was 20 mg/L. Because norfloxacin (NOR) competes for adsorption sites on the microplastic, CIP adsorption is inhibited. The adsorption model, FTIR, and XPS spectroscopy all indicated that CIP adsorption by microplastics was the result of a complex set of physicochemical interactions. Hydrogen bonding, π-π conjugation, ion exchange, and electrostatic interactions controlled the adsorption mechanism. These findings shed light on the mechanism of interaction between microplastics and antibiotics in water, as well as the ability of microplastic plastics in water to adsorb and transport CIP, providing the data required for ecological and environmental risk assessment of microplastic-antibiotic complex contamination.

Supplementary Information The online version contains supplementary material available at https://doi.org/10.1007/s11356-023-26390-x.

Author contribution Jinni Liang: conceptualization, methodology, software, data curation, writing – original draft preparation. Jiahui Wu: visualization, investigation. Zhi Zeng: validation. Manzhi Li:

validation. Weizhen Liu: investigation, visualization. Taiping Zhang: writing – reviewing and editing.

Funding This study was financially supported by the National Natural Science Foundation of China Projects (U21A2003) and The Guangdong Science and Technology program (No. 2020B121201003).

Data availability The data that supports the findings of this study are available within the article and its supplementary material.

Declarations

Ethical approval This study did not involve any human or animal experiments.

Consent to participate Not applicable.

Consent for publication Not applicable.

Conflict of interest We declare that we have no financial and personal relationships with other people or organizations that can inappropriately influence our work, and there is no professional or other personal interest of any nature or kind in any product, service, or company that could be construed as influencing the position presented in, or the review of, the manuscript entitled.

References

Alimi OS, Farner Budarz J, Hernandez LM, Tufenkji N (2018) Microplastics and nanoplastics in aquatic environments: aggregation, deposition, and enhanced contaminant transport. Environ Sci Technol 52:1704–1724. https://doi.org/10.1021/acs.est.7b05559

Andrady AL (2011) Microplastics in the marine environment. Mar Pollut Bull 62:1596–1605. https://doi.org/10.1016/j.marpolbul.2011.05.030

Ashiq A, Sarkar B, Adassooriya N, Walpita J, Rajapaksha AU, Ok YS et al (2019) Sorption process of municipal solid waste biochar-montmorillonite composite for ciprofloxacin removal in aqueous media. Chemosphere 236:124384. https://doi.org/10.1016/j.chemosphere.2019.124384

Atugoda T, Wijesekara H, Werellagama DRIB, Jinadasa KBSN, Bolan NS, Vithanage M (2020) Adsorptive interaction of antibiotic ciprofloxacin on polyethylene microplastics: implications for vector transport in water. Environ Technol Innov 19:100971. https://doi.org/10.1016/j.eti.2020.100971

Bakir A, Rowland SJ, Thompson RC (2014) Enhanced desorption of persistent organic pollutants from microplastics under simulated physiological conditions. Environ Pollut 185:16–23. https://doi.org/10.1016/j.envpol.2013.10.007

Bao ZZ, Chen ZF, Zhong Y, Wang G, Qi Z, Cai Z (2021) Adsorption of phenanthrene and its monohydroxy derivatives on polyvinyl chloride microplastics in aqueous solution: model fitting and mechanism analysis. Sci Total Environ 764:142889. https://doi.org/10.1016/j.scitotenv.2020.142889

Bhattacharyya KG, Sharma A (2004) Azadirachta indica leaf powder as an effective biosorbent for dyes: a case study with aqueous Congo Red solutions. J Environ Manage 71:217–229. https://doi.org/10.1016/j.jenvman.2004.03.002

Campanale C, Stock F, Massarelli C, Kochleus C, Bagnuolo G, Reifferscheid G et al (2020) Microplastics and their possible sources: the example of Ofanto river in southeast Italy. Environ Pollut 258:113284. https://doi.org/10.1016/j.envpol.2019.113284

Changfu Y, Jiani G, Yidi Y, Yijin L, Yiyao L, Yu F (2022) Interface behavior changes of weathered polystyrene with ciprofloxacin in seawater environment. Environ Res 212:113132. https://doi.org/10.1016/j.envres.2022.113132

Danner MC, Robertson A, Behrends V, Reiss J (2019) Antibiotic pollution in surface fresh waters: occurrence and effects. Sci Total Environ 664:793–804. https://doi.org/10.1016/j.scitotenv.2019.01.406

Ding J, Jiang F, Li J, Wang Z, Sun C, Wang Z et al (2019) Microplastics in the coral reef systems from Xisha Islands of South China Sea. Environ Sci Technol 53:8036–8046. https://doi.org/10.1021/acs.est.9b01452

Fan X, Zou Y, Geng N, Liu J, Hou J, Li D et al (2021) Investigation on the adsorption and desorption behaviors of antibiotics by degradable MPs with or without UV ageing process. J Hazard Mater 401:123363. https://doi.org/10.1016/j.jhazmat.2020.123363

Frias JP, Sobral P, Ferreira AM (2010) Organic pollutants in microplastics from two beaches of the Portuguese coast. Mar Pollut Bull 60:1988–1992. https://doi.org/10.1016/j.marpolbul.2010.07.030

Fu Z, Wu F, Song K, Lin Y, Bai Y, Zhu Y et al (2013) Competitive interaction between soil-derived humic acid and phosphate on goethite. Appl Geochem 36:125–131. https://doi.org/10.1016/j.apgeochem.2013.05.015

Gao F, Li J, Sun C, Zhang L, Jiang F, Cao W et al (2019) Study on the capability and characteristics of heavy metals enriched on microplastics in marine environment. Mar Pollut Bull 144:61–67. https://doi.org/10.1016/j.marpolbul.2019.04.039

Geyer R, Jambeck JR, Law KL (2017) Production, use, and fate of all plastics ever made. Sci Adv 3:e1700782. https://doi.org/10.1126/sciadv.1700782

Grenni P, Ancona V, Barra CA (2018) Ecological effects of antibiotics on natural ecosystems: a review. Microchem J 136:25–39. https://doi.org/10.1016/j.microc.2017.02.006

Guo X, Wang X, Zhou X, Kong X, Tao S, Xing B (2012) Sorption of four hydrophobic organic compounds by three chemically distinct polymers: role of chemical and physical composition. Environ Sci Technol 46:7252–7259. https://doi.org/10.1021/es301386z

Hasan MM, Kubra KT, Hasan MN, Awual ME, Salman MS, Sheikh MC et al (2023) Sustainable ligand-modified based composite material for the selective and effective cadmium(II) capturing from wastewater. J Mol Liq 371:121125. https://doi.org/10.1016/j.molliq.2022.121125

Horton AA, Svendsen C, Williams RJ, Spurgeon DJ, Lahive E (2017) Large microplastic particles in sediments of tributaries of the River Thames, UK – abundance, sources and methods for effective quantification. Mar Pollut Bull 114:218–226. https://doi.org/10.1016/j.marpolbul.2016.09.004

Huang X, Zemlyanov DY, Diaz-Amaya S, Salehi M, Stanciu L, Whelton AJ (2020) Competitive heavy metal adsorption onto new and aged polyethylene under various drinking water conditions. J Hazard Mater 385:121585. https://doi.org/10.1016/j.jhazmat.2019.121585

Jabar JM, Odusote YA (2020) Removal of cibacron blue 3G-A (CB) dye from aqueous solution using chemo-physically activated biochar from oil palm empty fruit bunch fiber. Arab J Chem 13:5417–5429. https://doi.org/10.1016/j.arabjc.2020.03.020

Jabar JM, Odusote YA (2021) Utilization of prepared activated biochar from water lily (Nymphaea lotus) stem for adsorption of malachite green dye from aqueous solution. Biomass Convers Biorefin. https://doi.org/10.1007/s13399-021-01399-9

Jabar JM, Adebayo MA, Owokotomo IA, Odusote YA, Yılmaz M (2022) Synthesis of high surface area mesoporous ZnCl2–activated cocoa (Theobroma cacao L) leaves biochar derived via pyrolysis for crystal violet dye removal. Heliyon 8:e10873. https://doi.org/10.1016/j.heliyon.2022.e10873

Jambeck JR, Geyer R, Wilcox C, Siegler TR, Perryman M, Andrady A et al (2015) Marine pollution. Plastic waste inputs from land into the ocean. Science 347:768–71. https://doi.org/10.1126/science.1260352

Jiang M, Hu L, Lu A, Liang G, Lin Z, Zhang T et al (2020) Strong sorption of two fungicides onto biodegradable microplastics with emphasis on the negligible role of environmental factors. Environ Pollut 267:115496. https://doi.org/10.1016/j.envpol.2020.115496

Kannaujiya MC, Kumar R, Mandal T, Mondal MK (2021) Experimental investigations of hazardous leather industry dye (Acid Yellow 2GL) removal from simulated wastewater using a promising integrated approach. Process Saf Environ Prot 155:444–454. https://doi.org/10.1016/j.psep.2021.09.040

Kannaujiya MC, Prajapati AK, Mandal T, Das AK, Mondal MK (2023) Extensive analyses of mass transfer, kinetics, and toxicity for hazardous acid yellow 17 dye removal using activated carbon prepared from waste biomass of Solanum melongena. Biomass Convers Biorefin 13:99–117. https://doi.org/10.1007/s13399-020-01160-8

Khandaker S, Chowdhury MF, Awual MR, Islam A, Kuba T (2021) Efficient cesium encapsulation from contaminated water by cellulosic biomass based activated wood charcoal. Chemosphere 262:127801. https://doi.org/10.1016/j.chemosphere.2020.127801

Klein EY, Van Boeckel TP, Martinez EM, Pant S, Gandra S, Levin SA et al (2018) Global increase and geographic convergence in antibiotic consumption between 2000 and 2015. Proc Natl Acad Sci U S A 115:E3463–E3470. https://doi.org/10.1073/pnas.1717295115

Li J, Zhang K, Zhang H (2018) Adsorption of antibiotics on microplastics. Environ Pollut 237:460–467. https://doi.org/10.1016/j.envpol.2018.02.050

Liu X, Lu S, Liu Y, Meng W, Zheng B (2017) Adsorption of sulfamethoxazole (SMZ) and ciprofloxacin (CIP) by humic acid (HA): characteristics and mechanism. RSC Adv 7:50449–50458. https://doi.org/10.1039/C7RA06231A

Lu Y, Zhang Y, Deng Y, Jiang W, Zhao Y, Geng J et al (2016) Uptake and accumulation of polystyrene microplastics in zebrafish (Danio rerio) and toxic effects in liver. Environ Sci Technol 50:4054–4060. https://doi.org/10.1021/acs.est.6b00183

Ma W, Xu X, An B, Zhou K, Mi K, Huo M et al (2021) Single and ternary competitive adsorption-desorption and degradation of amphenicol antibiotics in three agricultural soils. J Environ Manage 297:113366. https://doi.org/10.1016/j.jenvman.2021.113366

Naushad M, Alqadami AA, Al-Kahtani AA, Ahamad T, Awual MR, Tatarchuk T (2019) Adsorption of textile dye using para-aminobenzoic acid modified activated carbon: kinetic and equilibrium studies. J Mol Liq 296:112075. https://doi.org/10.1016/j.molliq.2019.112075

Polman E, Gruter GM, Parsons JR, Tietema A (2021) Comparison of the aerobic biodegradation of biopolymers and the corresponding bioplastics: a review. Sci Total Environ 753:141953. https://doi.org/10.1016/j.scitotenv.2020.141953

Qiao R, Lu K, Deng Y, Ren H, Zhang Y (2019) Combined effects of polystyrene microplastics and natural organic matter on the accumulation and toxicity of copper in zebrafish. Sci Total Environ 682:128–137. https://doi.org/10.1016/j.scitotenv.2019.05.163

Razanajatovo RM, Ding J, Zhang S, Jiang H, Zou H (2018) Sorption and desorption of selected pharmaceuticals by polyethylene microplastics. Mar Pollut Bull 136:516–523. https://doi.org/10.1016/j.marpolbul.2018.09.048

Sarici ÖzdemİrÇ (2018) Adsorptive removal of methylene blue by fruit shell: isotherm studies. Fullerenes, Nanotubes, Carbon Nanostruct 26:570–577. https://doi.org/10.1080/1536383X.2018.1472083

Shruti VC, Kutralam-Muniasamy G (2019) Bioplastics: missing link in the era of microplastics. Sci Total Environ 697:134139. https://doi.org/10.1016/j.scitotenv.2019.134139

Sighicelli M, Pietrelli L, Lecce F, Iannilli V, Falconieri M, Coscia L et al (2018) Microplastic pollution in the surface waters of Italian Subalpine Lakes. Environ Pollut 236:645–651. https://doi.org/10.1016/j.envpol.2018.02.008

Sun Y, Wang X, Xia S, Zhao J (2021) New insights into oxytetracycline (OTC) adsorption behavior on polylactic acid microplastics undergoing microbial adhesion and degradation. Chem Eng J 416:129085. https://doi.org/10.1016/j.cej.2021.129085

Sun M, Yang Y, Huang M, Fu S, Hao Y, Hu S et al (2022) Adsorption behaviors and mechanisms of antibiotic norfloxacin on degradable and nondegradable microplastics. Sci Total Environ 807:151042. https://doi.org/10.1016/j.scitotenv.2021.151042

Thompson RC, Moore CJ, Vom SF, Swan SH (2009) Plastics, the environment and human health: current consensus and future trends. Philos Trans R Soc Lond B Biol Sci 364:2153–2166. https://doi.org/10.1098/rstb.2009.0053

Wang J, Zhuan R, Chu L (2019) The occurrence, distribution and degradation of antibiotics by ionizing radiation: an overview. Sci Total Environ 646:1385–1397. https://doi.org/10.1016/j.scitotenv.2018.07.415

Xiong Y, Zhao J, Li L, Wang Y, Dai X, Yu F et al (2020) Interfacial interaction between micro/nanoplastics and typical PPCPs and nanoplastics removal via electrosorption from an aqueous solution. Water Res 184:116100. https://doi.org/10.1016/j.watres.2020.116100

Yang Y, Liu W, Xu C, Wei B, Wang J (2017) Antibiotic resistance genes in lakes from middle and lower reaches of the Yangtze River, China: effect of land use and sediment characteristics. Chemosphere 178:19–25. https://doi.org/10.1016/j.chemosphere.2017.03.041

Yousif E, Haddad R (2013) Photodegradation and photostabilization of polymers, especially polystyrene: review. Springerplus 2:398. https://doi.org/10.1186/2193-1801-2-398

Yu F, Yang C, Huang G, Zhou T, Zhao Y, Ma J (2020) Interfacial interaction between diverse microplastics and tetracycline by adsorption in an aqueous solution. Sci Total Environ 721:137729. https://doi.org/10.1016/j.scitotenv.2020.137729

Zhang H, Wang J, Zhou B, Zhou Y, Dai Z, Zhou Q et al (2018) Enhanced adsorption of oxytetracycline to weathered microplastic polystyrene: kinetics, isotherms and influencing factors. Environ Pollut 243:1550–1557. https://doi.org/10.1016/j.envpol.2018.09.122

Zheng M, Wu P, Li L, Yu F, Ma J (2023) Adsorption/desorption behavior of ciprofloxacin on aged biodegradable plastic PLA under different exposure conditions. J Environ Chem Eng 11:109256. https://doi.org/10.1016/j.jece.2022.109256

Zhou Y, Yang Y, Liu G, He G, Liu W (2020) Adsorption mechanism of cadmium on microplastics and their desorption behavior in sediment and gut environments: the roles of water pH, lead ions, natural organic matter and phenanthrene. Water Res 184:116209. https://doi.org/10.1016/j.watres.2020.116209

Zuo L, Li H, Lin L, Sun Y, Diao Z, Liu S et al (2019) Sorption and desorption of phenanthrene on biodegradable poly(butylene adipate co-terephtalate) microplastics. Chemosphere 215:25–32. https://doi.org/10.1016/j.chemosphere.2018.09.173